British Journal of Cancer (2012) 106, 1648–1659

www.bjcancer.com

Intrinsic resistance to selumetinib, a selective inhibitor of MEK1/2, by cAMP-dependent protein kinase A activation in human lung and colorectal cancer cells

T Troiani[1], L Vecchione[1,2], E Martinelli[1], A Capasso[1], S Costantino[3], LP Ciuffreda[3], F Morgillo[1], D Vitagliano[1], E D'Aiuto [4], R De Palma[4], S Tejpar[2], E Van Cutsem[2], M De Lorenzi[5,6], M Caraglia[7], L Berrino[3] and F Ciardiello*[,1]

[1]Oncologia Medica, Dipartimento Medico-Chirurgico di Internistica Clinica e Sperimentale F. Magrassi e A. Lanzara, Seconda Università degli Studi di Napoli, Via S. Pansini 5, Napoli 80131, Italy; [2]Department of Digestive Oncology, University Hospital Gasthuisberg, Herestraat 49 bus 602 Leuven 3000, Belgium; [3]Sezione di Farmacologia, Dipartimento di Medicina Sperimentale, Seconda Università degli Studi di Napoli, Via L. De Crecchio 7, Napoli 80138, Italy; [4]Immunologia Clinica, Dipartimento Medico-Chirurgico di Internistica Clinica e Sperimentale F. Magrassi e A. Lanzara, Seconda Università degli Studi di Napoli, Via S. Pansini 5, Napoli 80131, Italy; [5]Département de Formation et Recherche, Centre Hospitalier Universitaire Vaudois, Lausanne, Switzerland; [6]Swiss Institute of Bioinformatics, Lausanne, Switzerland; [7]Dipartimento di Biochimica and Biofisica, Via L. De Crecchio 7, Napoli 80138, Italy

BACKGROUND: MEK is activated in ~40% colorectal cancer (CRC) and 20–30% non-small cell lung cancer (NSCLC). Selumetinib is a selective inhibitor of MEK1/2, which is currently in clinical development.

METHODS: We evaluated the effects of selumetinib *in vitro* and *in vivo* in CRC and NSCLC cell lines to identify cancer cell characteristics correlating with sensitivity to MEK inhibition.

RESULTS: Five NSCLC and six CRC cell lines were treated with selumetinib and classified according to the median inhibitory concentration (IC_{50}) values as sensitive ($\leqslant 1\ \mu M$) or resistant ($>1\ \mu M$). In selumetinib-sensitive cancer cell lines, selumetinib treatment induced G1 cell-cycle arrest and apoptosis and suppression of tumour growth as xenografts in immunodeficient mice. Evaluation of intracellular effector proteins and analysis of gene mutations showed no correlation with selumetinib sensitivity. Microarray gene expression profiles revealed that the activation of cAMP-dependent protein kinase A (PKA) was associated with MEK inhibitor resistance. Combined targeting of both MEK and PKA resulted in cancer cell growth inhibition of MEK inhibitor-resistant cancer cell lines *in vitro* and *in vivo*.

CONCLUSION: This study provides molecular insights to explain resistance to an MEK inhibitor in human cancer cell lines.

British Journal of Cancer (2012) **106,** 1648–1659. doi:10.1038/bjc.2012.129 www.bjcancer.com

Keywords: selumetinib; PKA; gene expression; gene mutations; cancer cell resistance

The current approach to drug design in oncology is aimed at modulating specific cell signalling pathways that are important for tumour growth, survival, invasion, and metastasis (Hahn and Weinberg, 2002; Hanahan and Weinberg, 2011). In cancer cells, these pathways become deregulated resulting in aberrant signalling, inhibition of apoptosis, increased metastasis, and increased cell proliferation (Adjei and Hidalgo, 2005). Although normal cells integrate multiple signalling pathways for controlled growth and proliferation, tumours seem to be heavily reliant on activation of one or more pathways. It is conceivable that tumours that are 'driven' by a particular pathway will respond to therapeutics that target components of that pathway. One of the most challenging aspects of anticancer therapy is that patients may exhibit intrinsic or acquired drug resistance and, for most anticancer agents, despite intensive preclinical and clinical studies, the bases for drug resistance remain poorly understood. Therefore, it is crucial to identify biomarkers that may be used to predict cancer cell sensitivity to molecular targeted agents to recognise a molecular profile of patient's tumour to guide appropriate therapeutic choices (Downward, 2006).

The RAS/RAF/MEK/ERK signalling pathway is constitutively activated in several cancers, leading to uncontrolled cell proliferation, resistance to apoptosis and association with a more aggressive neoplastic phenotype (Sebolt-Leopold, 2004). Constitutive activation of the MAPK pathway may also contribute to cancer cell resistance to chemotherapy in several types of human malignancies, including pancreatic, colon, lung, thyroid, and breast cancers (Hoshino *et al*, 1999; Mueller *et al*, 2000). Signalling through this pathway occurs following activation of cell surface growth factor receptors by extracellular ligands, constitutive activation of cell surface growth factor receptors by gene mutation or protein overexpression, or through gain-of-function gene mutations of *BRAF* and *RAS* family members (Adjei, 2001). Activating mutations in *RAS* and *BRAF* typically shows mutual exclusivity in tumours, suggesting that the proteins encoded by these genes deregulate a common effector pathway. Mutations in *KRAS* gene occur in 40% colorectal cancer (CRC) and 20–30% of non-small cell lung cancer (NSCLC). Mutations in *KRAS* are associated with resistance to epidermal growth factor receptor (EGFR) inhibitors in CRC (Pao *et al*, 2005; Lievre *et al*, 2006;

*Correspondence: Dr F Ciardiello; E-mail: fortunato.ciardiello@unina2.it
Revised 8 March 2012; accepted 14 March 2012

Massarelli *et al*, 2007; Allegra *et al*, 2009; De Roock *et al*, 2010). The three RAF isoforms (RAF1, ARAF, and BRAF) activate both MEK1 and MEK2. Moreover, *BRAF* activating gene mutations are less common in CRC and NSCLC with incidence of 5–10% and $<5\%$, respectively (Brose *et al*, 2002; Yuen *et al*, 2002).

Selumetinib (AZD6244, ARRY-142886) is an oral, non-adenosine-5'-triphosphate (ATP) competitive inhibitor and is highly specific for MEK1/2. It is a potent, tight-binding, non-competitive MEK inhibitor with an median inhibitory concentration (IC_{50}) of 14.1 nmol L^{-1} against purified MEK1 with no observed inhibition at 10 μmol L^{-1} against >40 other serine/threonine kinases (Davies *et al*, 2007; Yeh *et al*, 2007). Selumetinib inhibits both basal and induced levels of ERK1/2 phosphorylation in numerous cancer cell lines such as colorectal, pancreatic, hepatocellular, non-small cell lung, and melanoma. It has also shown efficacy in different tumour models. Sustained inhibition of ERK activity in tumour can be achieved at a dose of 10 mg kg^{-1} per day in mice xenograft studies (Shannon *et al*, 2009). The safety profile and tolerability of selumetinib has been evaluated in a two-part, multi-centre, increasing dose, phase I clinical study (Adjei *et al*, 2008). This trial demonstrated the tolerability of selumetinib, with the most common related toxicities being rash, diarrhoea, nausea, and fatigue. Several studies are ongoing to evaluate the activity of selumetinib, as a single agent or in combination with chemotherapy in a variety of tumour types including CRC and NSCLC (Hainsworth *et al*, 2010; Bekaii-Saab *et al*, 2011; Bennouna *et al*, 2011; O'Nail *et al*, 2011).

Based on the role of the MAPK signalling pathway in CRC and NSCLC, the first objective of the present study has been to evaluate the sensitivity to selumetinib *in vitro* and *in vivo* in these two types of cancers by using a panel of different cancer cell lines. Following this initial screening, the goal of the present study has been to identify specific profiles for gene mutations, gene expression and/or intracellular signalling protein expression, which could allow to define different molecular patterns of either sensitivity or resistance to MEK inhibition in a model of 11 CRC and NSCLC cell lines.

MATERIALS AND METHODS

Drugs

The MEK1/2 inhibitor selumetinib was generously provided by Astra Zeneca (Macclesfield, UK). 8-cloro-cAMP (8-Cl-cAMP) was purchased from the BioLog Life Science Institute (Bremen, Germany). Synthesis of antisense 18-mer mixed backbone oligonucleotide (MBO) targeted to the 5′-terminal 8–13 codons of human RIα regulatory subunit messenger RNA of cAMP-dependent protein kinase A (PKAI) (Tortora *et al*, 1997a) was previously described (Agrawal *et al*, 1997). The PKAI antisense oligonucleotide, designated HYB 190, had the following sequence: 5′-GCGTGCCTCCTCACTGGC-3′ (Tortora *et al*, 1997a). A control PKAI antisense oligonucleotide containing four mismatched nucleotides was designated as HYB 239. The mismatched nucleotides in HYB 239 are underlined: 5′-GCATGCATCCGCA CAGGC-3′ (Tortora *et al*, 1997a). Both HYB 190 and HYB 239 contain phosphorothioate- and methylphosphonate-internucleotide linkages. The identity of each oligonucleotide was confirmed by ^{31}P nuclear magnetic resonance. Chemical purity of each MBO was determined by capillary gel electrophoresis, hybridisation melting temperature, and A_{269}/mass ratio (Agrawal *et al*, 1997).

Cell lines

Five human NSCLC cell lines (GLC82, A549, Calu3, H460, H1299) and six human CRC cell lines (GEO, HCT15, HCT116, SW480, SW620, LS174T) were obtained from the American Type Culture Collection (ATCC) (Manassas, VA, USA). All cancer cell lines, except GLC82, GEO, SW620, and LS174T, were cultured in RPMI-1640 medium (Invitrogen, Milan, Italy) supplemented with 10% fetal bovine serum (Lonza, Milan, Italy), 100 U ml^{-1} penicillin/streptomycin (Lonza) and were maintained in a humidified incubator. GLC82, GEO, SW620, and LS174T cancer cells were grown in McCoy medium (Lonza) supplemented with 20% fetal bovine serum (Lonza), 100 U ml^{-1} penicillin/streptomycin (Lonza). Cancer cell lines were tested by evaluating the mitochondrial DNA immediately after purchase from ATCC and then tested at various intervals to ensure that the mitochondrial DNA had not changed.

Proliferation assay

Cell proliferation was measured with the 3-(4, 5-dimethylthiazol-2-yl)-5-(3-carboxymethxyphenyl)-2-(4sulfophenyl)-2H-tetrazolium (MTT) assay. Briefly, cell suspensions (2000 μl) containing 10 000–15 000 viable cells were plated into each well and incubated for 48 h before exposure with different concentrations of selumetinib (0.01, 0.05, 0.25, 1, 5, and 10 μM), 8-Cl-cAMP (0.01, 0.05, 0.25,1, 2.5, and 5 μM), oligonucleotide HYB 190 (0.01, 0.05, 0.25,1, 2.5, and 5 μM), or oligonucleotide HYB 239 (0.01, 0.05, 0.25,1, 2.5, and 5 μM), as previously reported (Morgillo *et al*, 2011). Each experiment was done in triplicate. The IC_{50} values were determined by using the CurveExpert 1.3 software (Curve Expert, Mississippi, MS, USA) and plotted in a dose response curves. For the combination experiments, cancer cells were treated with different concentrations of selumetinib (0.01–5 μM) plus 8-Cl-cAMP (0.01–5 μM), HYB 190 (0.01–5 μM), or HYB 239 (0.01–5 μM) plus selumetinib each day, for a total of 3 days, at the fixed drug ratio selumetinib 8-Cl-cAMP of 1 : 1, and selumetinib HYB190 or HYB 239 of 1 : 1. The results of the combination treatment with selumetinib and 8-Cl-cAMP were analysed according to the method of Chou and Talalay by using the CalcuSyn software programme (Biosoft, Cambridge, UK).

Apoptotic assay and analysis of cell cycle

HCT116, HCT15, Calu3, and H460 cells were collected in six-well plates, treated for 24, 48, and 72 h with selumetinib (0.25 μM for HCT116, 0.05 μM for Calu3, and 10 μM for both HCT15 and H460) and stained with Annexin V–FITC. Apoptotic cell death was assessed by counting the numbers of cells that stained positive for Annexin V–FITC and negative for propidium iodide using an Apoptosis Annexin V–FITC Kit (Invitrogen), coupled with fluorescence-activated cell sorting analysis. Cell-cycle analysis was done by using flow cytometry on cell pellets that were fixed in 70% ethanol, washed in PBS, and mixed with RNase (Invitrogen) and propidium iodide (Invitrogen). Each experiment was done in triplicate. Student's *t*-test was used to evaluate the statistical significance of the results. All *P*-values represent two-sided tests of statistical significance. All analyses were done with the BMDP New System statistical package version 1.0 for Microsoft Windows (BMDP Statistical Software, Los Angeles, CA, USA).

Immunoblotting

HCT116, HCT15, Calu3, and H460 cells were seeded into 100 mm^3 dishes 24 h before treatment with selumetinib (0.05 μM). The analysis was done as previously described (Morgillo *et al*, 2011). We used the following antibodies from Cell Signalling Technology (Beverly, MA, USA): EGFR, phospho-EGFR (Tyr1068), MEK1/2, phospho-MEK1/2, p44/42 MAPK, phospho-p44/42MAPK, AKT, p-AKT (Ser473), 4E-BP1 and phospho-4E-BP1 (Thr37/46). The anti-human RIα mouse antibody was purchased from Transduction Laboratory (Lexington, NY, USA). The following secondary antibodies from Invitrogen were used: goat anti-rabbit IgG and rabbit anti-mouse IgG. Immunoreactive proteins were visualised by enhanced chemiluminescence (ECL plus; Amersham Italia, Milan, Italy). Each experiment was done in triplicate. Student's

t-test was used to evaluate the potential relationships expression of proteins and selumetinib response. The analysis was done with the BMDP New System statistical package version 1.0 for Microsoft Windows (BMDP Statistical Software).

Tumour xenografts in nude mice

Four- to six-week-old female balb/c athymic (nu+/nu+) mice were purchased from Charles River Laboratories (Milan, Italy). The research protocol was approved and mice were maintained in accordance with the institutional guidelines of the Second University of Naples Animal Care and Use Committee. The mice were injected subcutaneously with 2.5×10^6 HCT116, HCT15, Calu3, and H460 cancer cells that have been diluted in 200 μl of matrigel (BD Biosciences, Milan, Italy). Resulting xenograft tumours were measured daily until tumour volumes of 100–150 mm^3 were reached. Mice ($n = 10$ per group) were then randomised to treatment groups to receive vehicle control (10% ethanol/10% cremophor EL/80%), selumetinib (25 or 50 mg kg^{-1}; oral gavage), twice a day (BID), 8-Cl-cAMP (0.5 mg kg^{-1}; intraperitoneal injection) twice a week or the combination of both drugs for 21 days. The body weights were monitored daily. At doses of 25 or 50 mg kg^{-1} twice daily, selumetinib did not cause any apparent harm to the mice. Monitoring of tumour growth was continued until tumours reached 2000 mm^3, when mice were killed. Tumour size was evaluated twice per week by calliper measurements using the following formula: $\pi/6 \times$ larger diameter $\times$ (smaller diameter)^2. Student's *t*-test was used to evaluate the statistical significance of the results.

Microarray gene expression analysis of cancer cell lines

Agilent microarray analyses were done to assess baseline gene expression profile for each cancer cell line using a one colour labelling microarray system as described before (Morgillo *et al*, 2011). Data were extracted from slide image by using Agilent Feature Extraction software (v.10.5, Agilent Technology Italy, Milan, Italy). The raw data and associated sample information were loaded and processed by Gene Spring 11.5X (Agilent Technology Italy). For identification of genes significantly altered in resistant cells, total detected entities were filtered by signal intensity value (upper cutoff 100th and lower cutoff 20th percentile) and flag to remove very low signal entities. Data were analysed using Student's *t*-test ($P < 0.05$) with a Benjamini–Hochberg multiple test correction to minimise selection of false positives. Of the significantly differentially expressed RNA, only those with greater than two-fold increase or two-fold decrease as compared with the controls were used for further analysis. Subsequently, hierarchical clustering (condition tree) was applied to the data files. In this way, the relationships between the different groups are shown. The condition tree was displayed as a heat map, based on the expression levels of the probe sets. Functional and network analyses of statistically significant gene expression changes were performed using Ingenuity Pathways Analysis (IPA) 8.0 (Ingenuity Systems, http://www.ingenuity.com). Analysis considered all genes from the data set that met the two-fold (*P*-value < 0.05) change cut-off and that were associated with biological functions in the Ingenuity Pathways Knowledge Base. The significance of the association between the data set and the canonical pathway was measured in two ways: (1) Ratio of the number of genes from the data set that map to the pathway divided by the total number of genes that map to the canonical pathway is displayed and (2) Fisher's exact test was used to calculate a *P*-value determining the probability that the association between the genes in the data set and the canonical pathway is explained by chance alone.

Evaluation of gene mutations

All cell lines were plated in 100 mm^3 dishes and after 24 h DNA was extracted using the DNAeasy Mini Kit (Qiagen Inc., Milan, Italy)

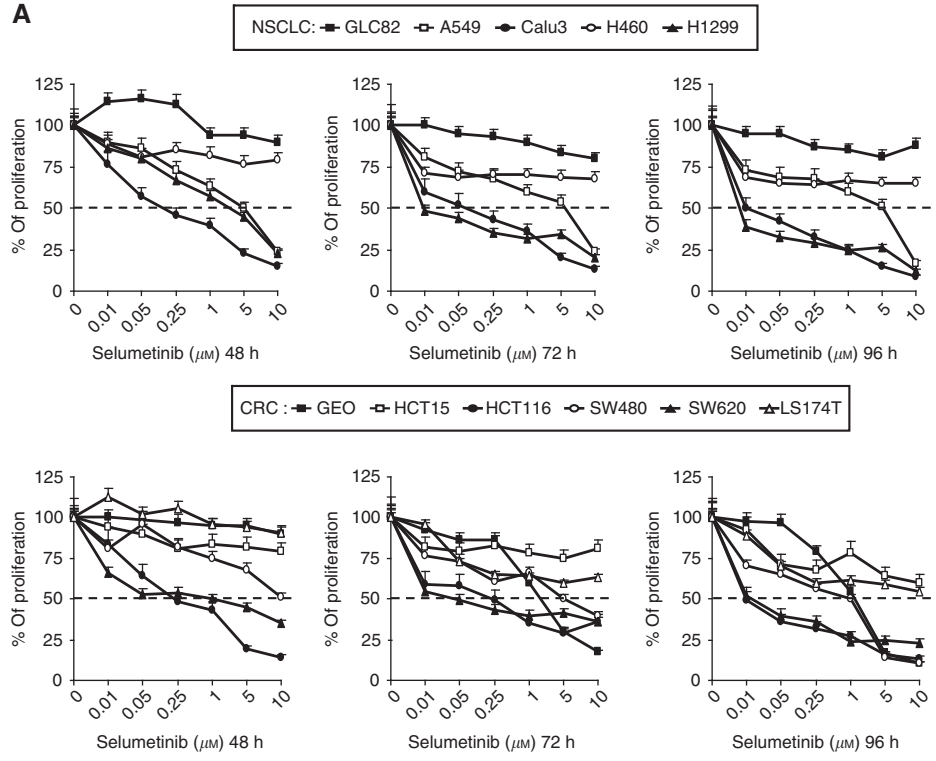

B

NSCLC	Selumetinib$_{(IC50)}$ 96 h	Sensitivity
GLC82	>10	R
H460	>10	R
A549	5	R
H1299	<0.01	S
Calu3	<0.01	S

CRC	Selumetinib$_{(IC50)}$ 96 h	Sensitivity
HCT15	>10	R
LS174T	10	R
GEO	1	S
SW480	1	S
HCT116	0.01	S
SW620	0.01	S

Figure 1 Effects of selumetinib on cell proliferation in the panel of human (**A**) NSCLC and (**B**) CRC cell lines. Cells were treated with increasing concentrations of selumetinib (0.01–10 μM) for 48, 72, and 96 h and evaluated for proliferation by MTT staining, as described in Materials and Methods. The results are average ± s.d. of three independent experiments each done in duplicate.

following manufacturer's instructions. We used the COSMIC database (Wellcome Trust Sanger Institute, Catalogue of somatic mutations in cancer. http://www.sanger.ac.uk/genetics/CGP/cosmic, accessed 15 October 2008) for mutations in *KRAS, NRAS, BRAF, PIK3CA, p53, PTEN, MAP2K4 (MEK), AKT, EGFR,* occurring in lung and CRC and selected the most frequent mutations per gene. Genomic positions of the mutated nucleotides were downloaded from Ensembl, and 200 bp upstream and downstream sequences were used for primer design with the Sequenom Mass ARRAY, Assay Design 3.1 software (Sequenom, Inc., Hamburg, Germany) using default parameters. Multiplex PCR was performed in a 5-μl volume containing 0.5 units of Hotstar Taq polymerase, 5–10 ng of genomic DNA, 100 nM of each PCR primer, and 500 μM of dNTP. Thermocycling was performed at 95 °C for 15 min, followed by 45 cycles of 94 °C for 20 s, 56 °C for 30 s and 72 °C for 60 s, followed by a final extension of 72 °C for 3 min. Unincorporated dNTPs were deactivated using 0.3 units of shrimp alkaline phosphatase at 37 °C for 40 min and primer extension was carried out using 7–14 μM of each primer extension probe (depending on the mass), 1 unit of iPLEX termination mix, and 1 unit of iPLEX enzyme. Reactions were cycled at 94 °C for 30 s, followed by 40 cycles of 94 °C for 5 s, 52 °C for 5 s and 80 °C for 5 s, followed by a final extension at 72 °C for 3 min. After the addition of a cation exchange resin to remove residual salt from the reactions, 20 μl of water was added and the extension product was spotted onto a matrix pad (3-hydroxypicoloinic acid) of a Spectro CHIP (Sequenom). After analysing the Spectro CHIPs using a Bruker MALDI-TOF mass spectrometer, spectra were processed by the Spectro READER software (Sequenom) and transferred to the Mass ARRAYTyper 4 Analyser (Sequenom) for further analysis. Genotyping for every sample was performed using the default settings of the Mass ARRAYTyper 4 Analyser. Automated genotyping calls were generated using the Mass ARRAY. The sensitivity of Sequenom gene mutation detection was between 5% and 15% and was determined by using DNA from different cell lines. Fisher's exact test was used to determine potential relationships between mutational status and selumetinib response.

RESULTS

In-vitro inhibition of cell proliferation by selumetinib treatment in NSCLC and CRC cell lines

We first evaluated the sensitivity to the selective MEK1/2 inhibitor, selumetinib, in a panel of five NSCLC (GLC82, H460, A549, H1299, Calu3) and six CRC (GEO, HCT15, HCT116, SW480, SW620, LS174T) cell lines by using the MTT assay. Cancer cells were treated with selumetinib at concentrations ranging from 0.01 to 10 μM for 48, 72, and 96 h. As shown in Figure 1, there was a wide range of sensitivity, with IC_{50} values varying between 0.01 and >10 μM. We classified as sensitive (S) or resistant (R) the cancer cell lines according to selumetinib IC_{50} at 96 h $\leqslant 1$ or >1 μM, respectively. This concentration was chosen based on the data from phase I studies, which indicated that 1 μM was within the average plasma concentrations of selumetinib achieved in patients at the maximum tolerated dose for this agent (Adjei *et al,* 2008). Overall, 67% (four of six) CRC and 40% (two of five) NSCLC cell

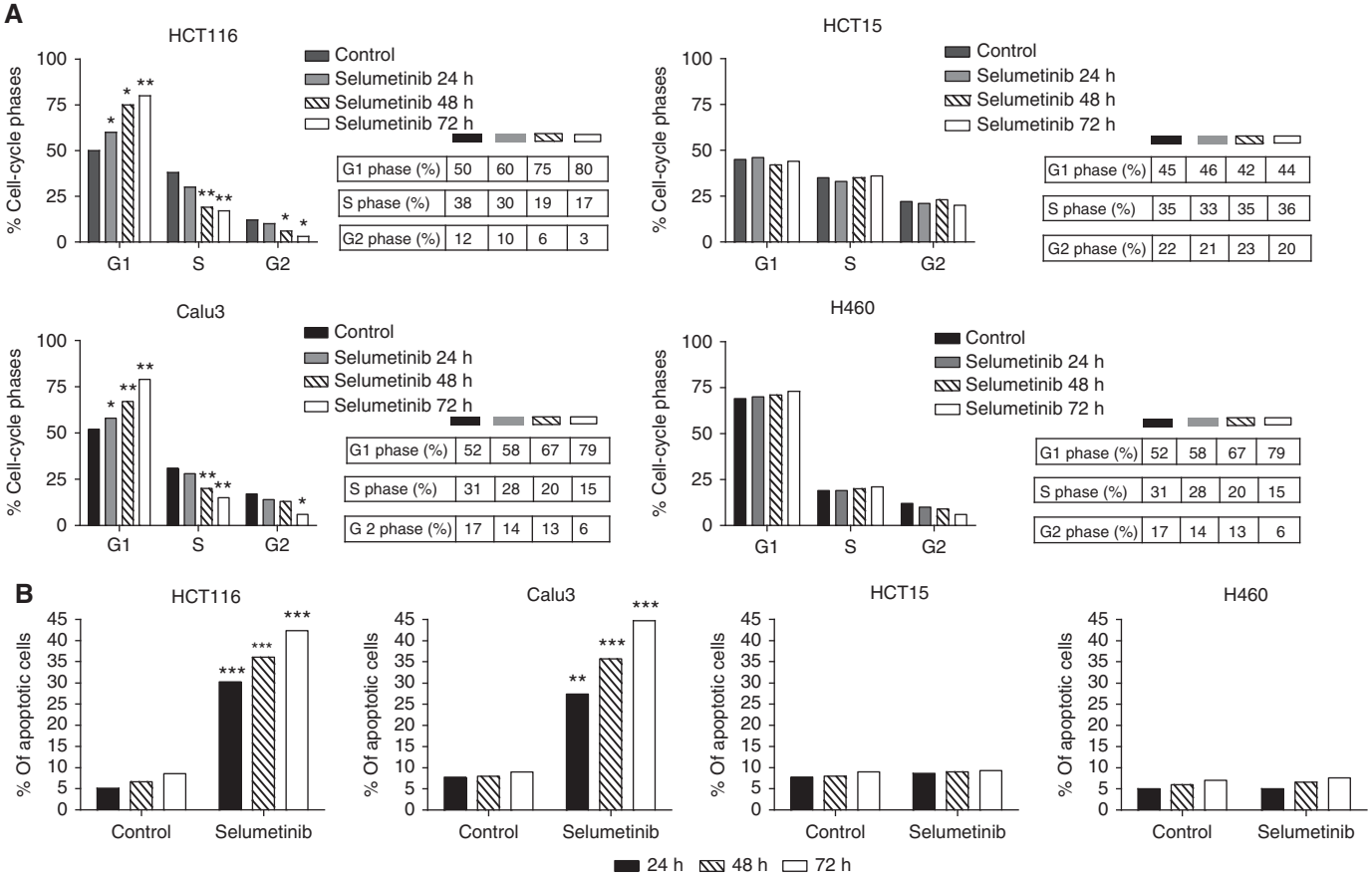

Figure 2 Effects of selumetinib treatment on cell-cycle distribution (**A**) and on apoptotic induction (**B**). HCT116, HCT15, Calu3, and H460 were treated with selumetinib (0.25 μM for HCT116, 0.05 μM for Calu3, and 10 μM for both HCT15 and H460) for 24, 48, and 72 h. (**A**) Flow cytometric analysis of cell-cycle distribution was performed as described in Materials and Methods. Percentages of cells in G1, S, and G2 phases of the cell cycle are shown. (**B**) Apoptosis was evaluated with Annexin V staining, as described in Materials and Methods. The rate of apoptosis was expressed as a percentage of the total cells counted. Columns, means of three independent experiments; $*P<0.05$; $**P<0.005$; $***P<0.0005$.

lines had a selumetinib IC_{50} of $\leqslant 1\,\mu M$. In particular, among the sensitive cancer cell lines there were four, two NSCLC (Calu3 and H1299) and two CRC (HCT116 and SW620), extremely sensitive to selumetinib with an IC_{50} of $\leqslant 0.01\,\mu M$ (Figure 1A and B). To investigate the mechanisms underlying the different sensitivities to the drug, we conducted experiments on a group of four cancer cell lines representing both selumetinib-sensitive (HCT116 and Calu3) and selumetinib-resistant (HCT15 and H460) models.

Effects of selumetinib treatment on cell-cycle distribution in NSCLC and CRC cell lines

We conducted flow cytometric analysis to compare the cell-cycle distribution following treatment of the selumetinib-sensitive HCT116 and Calu3 cancer cell lines and of the selumetinib-resistant HCT15 and H460 cancer cell lines. Cancer cells were treated with selumetinib at the IC_{50} values for inhibition of cell proliferation for 24, 48, and 72 h. Twenty-four hours selumetinib treatment caused cell accumulation in the G1 phase and concomitant reduction in the S phase as compared with controls in selumetinib-sensitive cancer cell lines (Figure 2A). The arrest in the G1 phase was significantly increased with longer (48 and 72 h) treatment with selumetinib in both HCT116 and Calu3 cells. This effect was also paralleled by a time-dependent reduction in the S phase in both selumetinib-sensitive cancer cell lines (Figure 2A). In contrast, no effect was observed on cell-cycle distribution in the two selumetinib-resistant HCT15 and H460 cells (Figure 2A). These results were supported also by Garon *et al* (2010), in which the block in G1 phase inducted by selumetinib is evident only in sensitive cell lines.

Effects of selumetinib treatment on the induction of apoptosis in NSCLC and CRC cell lines

Several preclinical models have demonstrated that selumetinib act as a cytotoxic drug rather than cytostatic by inducing proapoptotic activity (Huynh *et al*, 2007a; Huynh *et al*, 2007b; Meng *et al*, 2009; Meng *et al*, 2010). To confirm this effect, the induction of apoptosis was evaluated using an FACS-based assay for Annexin V and PI staining. After 24 h of selumetinib treatment, a significant induction of apoptosis was detected in the sensitive HCT116 and Calu3 cancer cell lines, which was maximal following 72 h of treatment (Figure 2B). Moreover, apoptosis was not detectable following treatment with selumetinib in the two resistant HCT15 and H460 cancer cell lines (Figure 2B).

Effects of selumetinib treatment on intracellular signalling in NSCLC and CRC cell lines

To assess the effects of selumetinib treatment on key intracellular downstream signalling pathways, western blots were performed to assess total and phosphorylated EGFR and downstream effectors (total MEK1/2, phospho-MEK1/2, total MAPK, phospho-MAPK, total AKT, phospho-AKT, total 4EBP1, and phosho-4EBP1). Cancer cells were evaluated at baseline and at different time points after treatment with selumetinib at $0.05\,\mu M$. No change in total and phosphorylated EGFR expression was observed in both selumetinib-sensitive and selumetinib-resistant cancer cell lines (Figure 3A–D). Treatment with selumetinib caused a time-dependent inhibition in phospho-MEK1/2 with a complete signal suppression within 60 or 15 min of treatment in HCT116 and Calu3 cells, respectively (Figure 3A and B). This inhibition was sustained

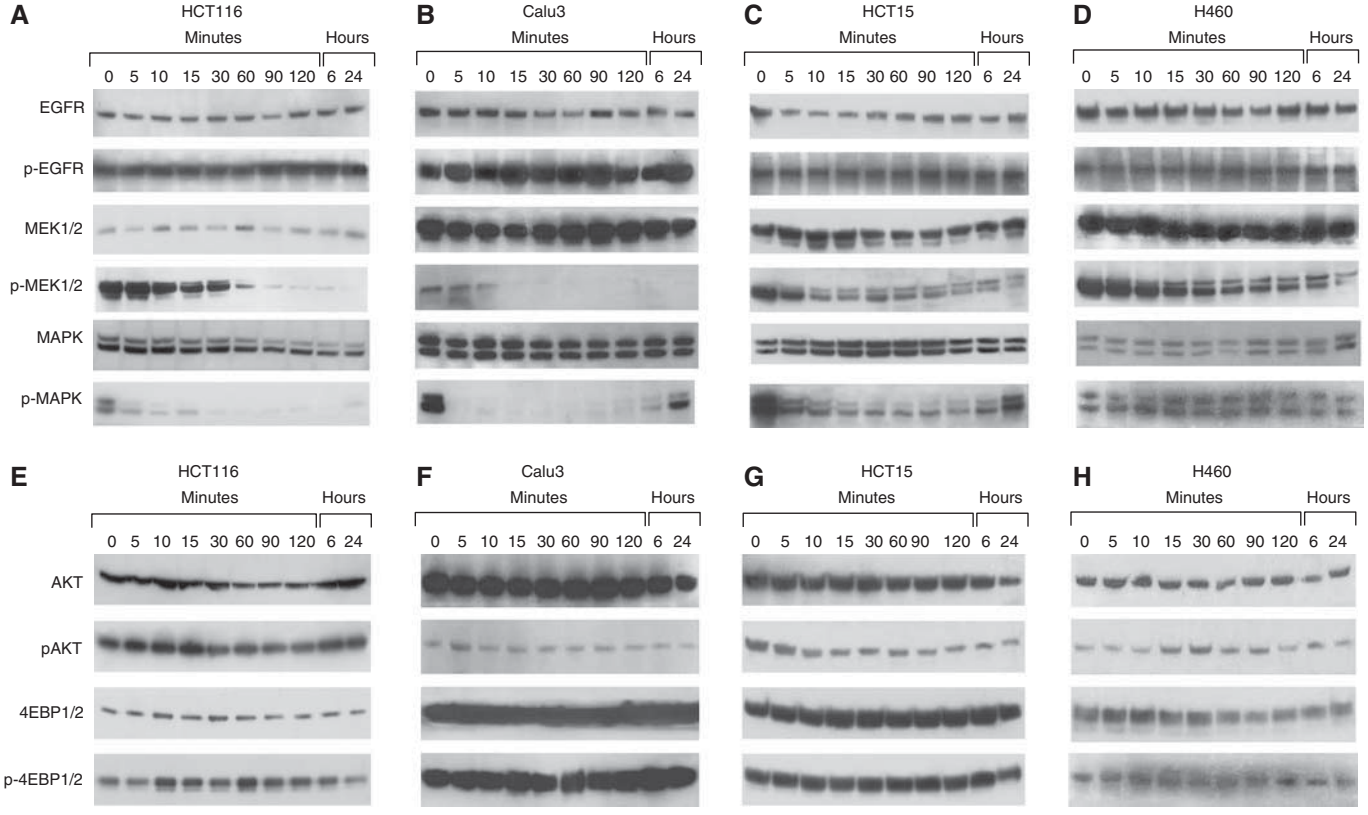

Figure 3 (**A**–**H**). Western blot analysis of intracellular signalling proteins in selumetinib-sensitive and selumetinib-resistant CRC and NSCLC cell lines. Analysis of intracellular signalling pathways was done by western blotting in two sensitive (HCT116 and Calu3) and two resistant (HCT15 and H460) cancer cells treated with $0.05\,\mu M$ selumetinib for the indicated time periods. Total cell protein extracts were fractionated through 4–12% SDS–PAGE, transferred onto nitrocellulose filters, and incubated with the appropriate antibodies as described in Materials and Methods. Immunoreactive proteins were visualised by enhanced chemiluminescence. Experiments were repeated three times with similar results.

for 24 h of selumetinib treatment in both cancer cell lines. In contrast, MEK1/2 inhibition of protein phosphorylation was less effective with only a slight reduction in pospho-MEK1/2 in the two selumetinib-resistant HCT15 and H460 cancer cell lines (Figure 3C and D). Moreover, MAPK phosphorylation was completely blocked following selumetinib treatment in HCT116 and Calu3. In contrast, in the two selumetinib-resistant HCT15 and H460 cells MAPK phosphorylation was only reduced but never completely abrogated (Figure 3C and D). We next assessed the levels of AKT, phosphor-AKT, 4EBP1 and poshospho-4EBP1, which are downstream effectors of the PI3 kinase (PI3K) pathway. Previous reports have suggested that resistance to selumetinib treatment in CRC and NSCLC cell lines was associated with baseline increased PI3K signalling (Balmanno *et al*, 2009). However, as depicted in Figure 3E–H, we failed to segregate the panel of 11 NSCLC and CRC cell lines into selumetinib-sensitive and selumetinib-resistant groups, by using the PI3K pathway.

Effects of selumetinib treatment on NSCLC and CRC tumour xenografts in nude mice

As shown in Figure 4A and B, HCT116 and Calu3 xenograft growth was significantly inhibited by selumetinib treatment in a dose-dependent manner. As an example, at day 50 from the injection of cancer cells, the mean tumour volume in mice bearing HCT116 tumour xenografts and treated with selumetinib, 25 or 50 mg kg^{-1} were 40% and 15%, respectively, as compared with control untreated mice. Similarly, at day 50 from the injection of cancer cells, the mean tumour volume in mice bearing Calu3 tumour xenografts and treated with selumetinib, 25 or 50 mg kg^{-1} were 22% and 8%, respectively, as compared with control untreated mice. In contrast, selumetinib treatment was unable to affect tumour growth in both HCT15 and H460 tumour xenografts (Figure 4C and D).

EGFR, RAS, MEK, and AKT protein expression and selumetinib sensitivity in NSCLC and CRC cell lines

Identification of predictive biomarkers is becoming a fundamental aspect in the development of targeted agents. So far, several preclinical studies have been published trying to address this aspect for the sensitivity to MEK inhibitors, but, since different results have been reported, no univocal interpretation could be made (Balmanno *et al*, 2009; Dry *et al*, 2010; Garon *et al*, 2010; Tendler *et al*, 2010). To identify specific profiles, which could allow identifying different molecular patterns of sensitivity or resistance to MEK inhibition, we first screened the intracellular signalling status of each cell lines. As depicted in Supplementary Figure 1A, the NCSLC and CRC cell lines displayed highly variable basal levels of total and phosphorylated EGFR, RAS, MEK, and AKT. As illustrated in Supplementary Figure 1B, there was no apparent correlation between basal levels of total and phosphorylated proteins listed above in both tumour types.

Gene mutations and selumetinib sensitivity in NSCLC and CRC cell lines

Activation of the classic MAPK cascade (RAS-RAF-MEK-ERK) is a common event in colorectal and lung cancer. Some genes within this pathway are mutated or aberrantly expressed. Moreover, the MAPK pathway can be indirectly activated by mutations of genes encoding for PI3K/PTEN/AKT and p53. We have screened the panel of 11 NSCLC and CRC cell lines for mutations in *KRAS, NRAS, BRAF, PIK3CA, p53, PTEN, MEK1/2, AKT, EGFR*

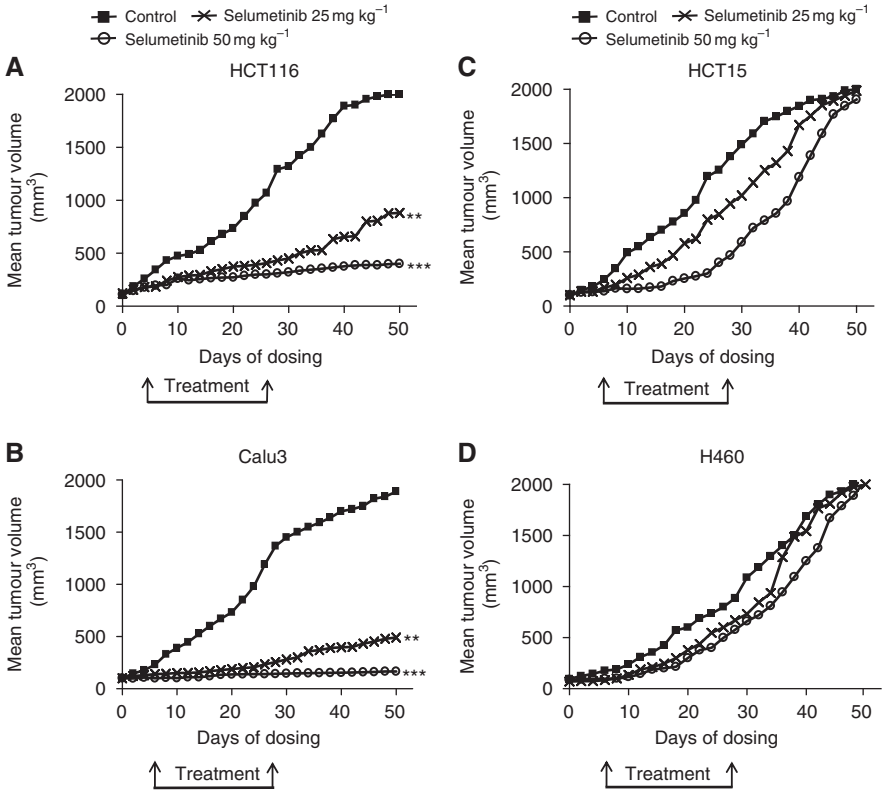

Figure 4 Effects of selumetinib on human CRC and NSCLC xenografts. Mice bearing (**A**) HCT116, (**B**) Calu3, (**C**) HCT15, and (**D**) H460 cancer cells were treated with vehicle or selumetinib (25 or 50 mg kg^{-1}, oral, BID) for 21 days ($n = 10$ mice per group). Treatments started when tumour reached volumes of 100–150 mm^3. Animals were killed when tumour reached 2000 mm^3 in size. ** $P < 0.005$; *** $P < 0.0005$.

Table 1 Mutation status and sensitivity to selumetinib in a panel of NSCLC and CRC cell lines

Cell line	Gene	Amino-acid change	Sensitivity
GLC82	*PIK3CA*	p.H1047R	R
H460	*PIK3CA*	p.E545K	R
	KRAS	p.Q61H	
A549	*KRAS*	p.G12S	R
	PIK3CA	p.Q546K	
H1299	*NRAS*	p.Q61K	S
Calu3	—	—	S
HCT15	*KRAS*	p.G13D	R
	PIK3CA	p.E545K	
LS174T	*KRAS*	p.G12D	R
	PIK3CA	p.H1047R	
GEO	*KRAS*	p.G12A	S
SW480	*KRAS*	p.G12V	S
HCT116	*KRAS*	p.G13D	S
	PIK3CA	p.H1047R	
SW620	*KRAS*	p.G12V	S

Abbreviations: CRC = colorectal cancer; NSCLC = non-small cell lung cancer; R = resistant; S = sensitive; — = no mutations.

(Table 1; Supplementary Table 1A–F). In NSCLC cell lines, two out of five (40%) harboured a *KRAS* mutation, which was located in codon 12 or 13. Moreover, three out of five (60%) of NSCLC cells harboured a *PI3KCA* mutation, which were located in exon 9 or 20. A concomitant mutation in *KRAS* and *PI3KCA* gene was found in two out of five (40%) NSCLC. One NSCLC cell line had an *NRAS* mutation (Table 1; Supplementary Table 1A–F). In the panel of six CRC cell lines, all of them harboured a *KRAS* gene mutation that was located in codon 12 or 13. Moreover, half of CRC cell lines had both a *PI3KCA* mutation in exon 9 or 20 and a *KRAS* mutation. None of the CRC cells had an *NRAS* mutation. No *BRAF* mutations were observed in the whole panel of NSCLC and CRC cells. As reported in Supplementary Table 1E and F, no other gene mutations were found in both NSCLC and CRC cell lines. After this screening, we tried to correlate the mutational status with selumetinib sensitivity. The analysis was made either considering separately the two sets of cell lines (data not shown) or all together (Supplementary Figure 2A and B). Sensitivity to selumetinib did not seem to correlate with any specific gene mutations in this panel of NSCLC and CRC cell lines.

Identification of gene expression profiles that could be predictive of response to selumetinib in NSCLC and CRC cell lines

RNAs from the 11 cancer cell lines were extracted and used for microarray gene expression analysis. Using Student's *t*-test with Benjamini–Hochberg multiple test correction, 21 and 18 genes were identified as upregulated or downregulated, respectively, in selumetinib-resistant cancer cell lines (*t*-test, $P<0.05$) (Supplementary Figure 3). Table 2 lists the differentially expressed genes in selumetinib-resistant cancer cell lines. Among the 21 genes that were upregulated in selumetinib-resistant cancer cell lines, we identified two genes, *ADCY7* and *AKAP13,* which are involved in the cAMP-dependent protein kinase (PKA) pathway (Table 2A; Supplementary Figure 3). The *ADCY7* gene encodes a membrane-bound adenylatecyclase that convert ATP into 3', 5'-adenosine monophosphate (cAMP) and pyrophosphate (Supplementary Figure 4). The cAMP is a second messenger that has a key role in intracellular signalling transduction. A major function in mammalian cells is the activation of the PKA (Tasken *et al,* 1997). The *AKAP13* gene encodes the A-kinase anchor protein 13 that has the function of binding to the regulatory subunits of PKA (Supplementary Figure 4). Moreover, four genes (*NCOA3, TAF3, NR1H2*, and *RXRA*), which are upregulated in selumetinib-resistant cancer cell lines, belong to the retinoic acid pathway, which is also activated by PKA (Altucci *et al,* 2007).

Table 2 List of the genes that are upregulated (A) and downregulated (B) in selumetinib-resistant CRC and NSCLC cell lines

Gene symbol	Gene name	FC	*P*-value
(A)			
LGALS8	Lectin, galactoside-binding, soluble, 8	17265	0.000759
TBX3	T-box 3	9565	0.00085
RHOBTB1	Rho-related BTB domain containing 1	534	0.010506
EFNA1	Ephrin-A1	5065	0.00475
CD14	CD14 molecule	4655	0.015522
RGP1	RGP1 retrograde golgi transport homologue (*S. cerevisiae*)	459	0.0035
CKAP4	Cytoskeleton-associated protein 4	432	0.000852
AKAP13	A kinase (PRKA) anchor protein 13	3955	0.00117
RXRA	Retinoid X receptor, alpha	3935	0.00101
VASN	Vasorin	3865	0.00355
ADCY7	Adenylate cyclase 7	3835	0.004585
ZNF516	Zinc finger protein 516	348	0.003229
TAF3	TAF3 RNA polymerase II, TATA box binding protein (TBP)-associated factor, 140 kDa	3235	0.001045
ZNF618	Zinc finger protein 618	322	0.0168
NCOA3	Nuclear receptor co-activator 3	306	0.020052
BRWD1	Bromodomain and WD repeat domain containing 1	2955	0.023051
AHCYL2	Adenosylhomocysteinase-like 2	2855	0.01875
TAOK1	TAO kinase 1	274	0.0035
NLK	Nemo-like kinase	266	0.000501
FTL	Ferritin, light polypeptide	232	0.0033
NR1H2	Nuclear receptor subfamily 1, group H, member 2	232	0.00385
(B)			
TNIK	TRAF2 and NCK interacting kinase	−1707	0.0065
SH3TC2	SH3 domain and tetratricopeptide repeats 2	−9605	0.005501
SOBP	Sine oculis binding protein homologue (*Drosophila*)	−577	0.006542
S100A2	S100 calcium binding protein A2	−5635	0.016571
FERMT1	Fermitin family homologue 1 (*Drosophila*)	−5335	0.00084
EMILIN2	Elastin microfibril interfacer 2	−515	0.024016
GNL1	Guanine nucleotide binding protein-like 1	−347	0.015001
HNRNPD	Heterogeneous nuclear ribonucleoprotein D (AU-rich element RNA binding protein 1)	−3275	0.00345
INF2	Inverted formin, FH2 and WH2 domain containing	−3175	0.0072
KLF6	Kruppel-like factor 6	−2985	0.016502
SMTN	Smoothelin	−297	0.024001
KRR1	KRR1, small subunit (SSU) processome component, homologue (yeast)	−2705	0.014356
MXD1	MAX dimerisation protein 1	−27	0.0257
RAB3IP	RAB3A interacting protein (rabin3)	−2525	0.01735
SMAGP	Small cell adhesion glycoprotein	−2325	0.006003
FAM82B	Family with sequence similarity 82, member B	−2265	0.002593
ZNF180	Zinc finger protein 180	−2245	0.01795
RPS6KA4	Ribosomal protein S6 kinase, 90 kDa, polypeptide 4	−2125	0.0229

Abbreviations: CRC = colorectal cancer; NSCLC = non-small cell lung cancer.

Treatment with selective PKA inhibitors sensitises selumetinib-resistant cancer cell lines to selumetinib

To functionally evaluate if the cAMP-dependent PKA could mediate resistance to MEK inhibitor treatment, we have treated the panel of NSCLC and CRC with 8-Cl-cAMP, a site-selective cAMP analogue, which specifically inhibits PKAI, the PKA isoform that is directly involved in mitogenic signalling and the transformed phenotype (Tortora and Ciardiello, 2000; Naviglio *et al*, 2009). A dose-dependent inhibition of growth was observed

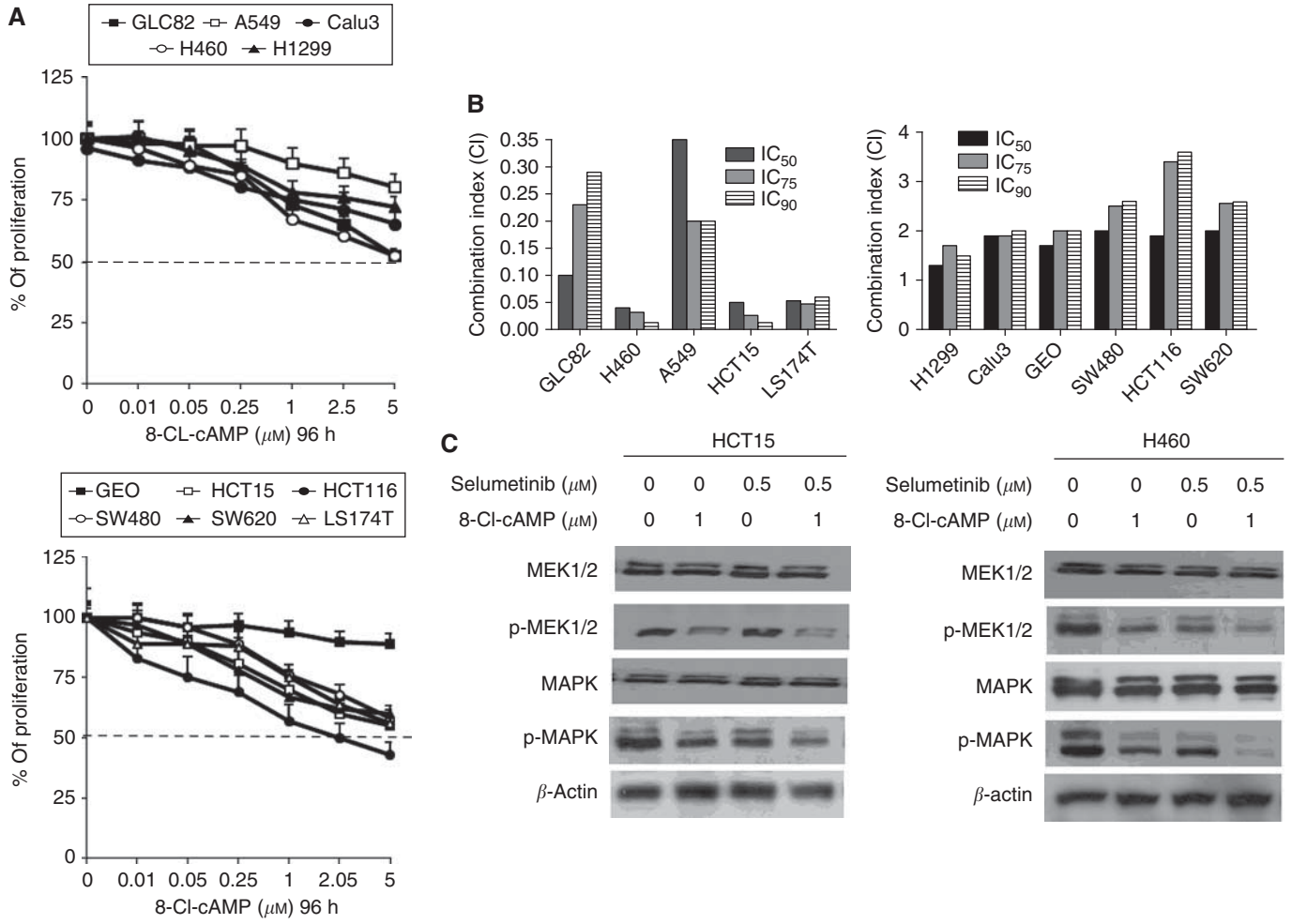

Figure 5 8-Cl-cAMP treatment restores cancer cell sensitivity to MEK inhibition. (**A**) Cancer cells were treated with increasing concentrations of 8-Cl-cAMP (range, 0.01–5 μM) for 96 h and evaluated for proliferation by MTT staining, as described in Materials and Methods. The results are average ± s.d. of three independent experiments each done in duplicate. (**B**) Cancer cells were treated with different concentrations of selumetinib plus 8-Cl-cAMP as described in Materials and Methods. Experiments were done in triplicate. CI values were calculated according to Chou and Talalay model for drug interactions using the CalcuSyn software. (**C**) HCT15 and H460 cancer cells were treated with selumetinib, 8-Cl-cAMP or selumetinib in combination with 8-Cl-cAMP at the indicated concentrations for 30 min. The cell lysates were immunoblotted with the indicated antibodies, as described in Materials and Methods.

in all cancer cell lines with a different degree of sensitivity, as illustrated in Figure 5A.

To evaluate the interaction between selumetinib and 8-Cl-cAMP, combination analyses were done. The CRC and NSCLC cancer cells were treated with different concentrations of selumetinib (range, 0.01–10 μM) and 8-Cl-cAMP (range, 0.01–5 μM) each day, for a total of 3 days at a fixed drug ratio selumetinib to 8-Cl-cAMP of 1 : 1. In all selumetinib-resistant cancer cell lines, the combination treatment caused synergistic growth inhibitory effects. In fact, the CI values for the combinations treatments ranged between 0.013 and 0.350. This was significantly different in the selumetinib-sensitive cancer cells in which the combination treatment was clearly antagonistic with CI between 1.3 and 3.6 (Figure 5B).

We next assessed the phosphorylation state of MEK and MAPK following treatment with selumetinib, 8-Cl-cAMP as single agents or in combination with HCT15 and H460 cancer cell lines. As shown in Figure 3C, single agent selumetinib or 8-Cl-cAMP slightly inhibited p-MEK and p-MAPK, whereas the combination induced a significant inhibition of both phosphorylated proteins.

A genetic approach to inhibiting PKAI expression was developed by the use of phosphorothioate antisense oligonucleotides targeting the synthesis of the PKAI regulatory subunit RIα. These oligonucleotides inhibit growth of several human cancer cell lines *in vitro* and *in vivo* (Yokozaki *et al*, 1993; Nesterova and Cho-Chung, 1995; Tortora *et al*, 1997a). Therefore, HYB 190, an 18-mer MBO antisense to the N-terminal 8–13 codons of the RIα subunit of PKAI, and the control HYB 239, containing four mismatched bases, were tested to study the effect on the growth of NSCLC and CRC cell lines. All cancer cell lines treated with HBY 190 displayed a dose-dependent inhibition of growth by MTT assay (Figure 6A). Growth inhibition was more pronounced in selumetinib-resistant cancer cell lines (IC_{50} between 0.25 and 1 μM), while the IC_{50} values were >5 μM in the selumetinib-sensitive cancer cells. In contrast, the control oligonucleotide, HYB 239, at doses up to 5 μM, showed only 5–15% growth inhibition among all of the cell lines tested (Figure 6A). To determine whether a combination of selumetinib and oligonucleotide HYB 190 could enhance the antiproliferative effect compared with either agent alone, selumetinib-resistant cells were treated with different combinations of the two agents at a fixed drug ratio of 1 : 1. As shown in Figure 6B, the combination treatment caused synergistic growth inhibitory effects. To determine whether the growth inhibitory effect of oligonucleotide HYB 190 correlated with a reduction in RIα protein levels, we performed protein blots on total cell extracts prepared from H460 cells treated with

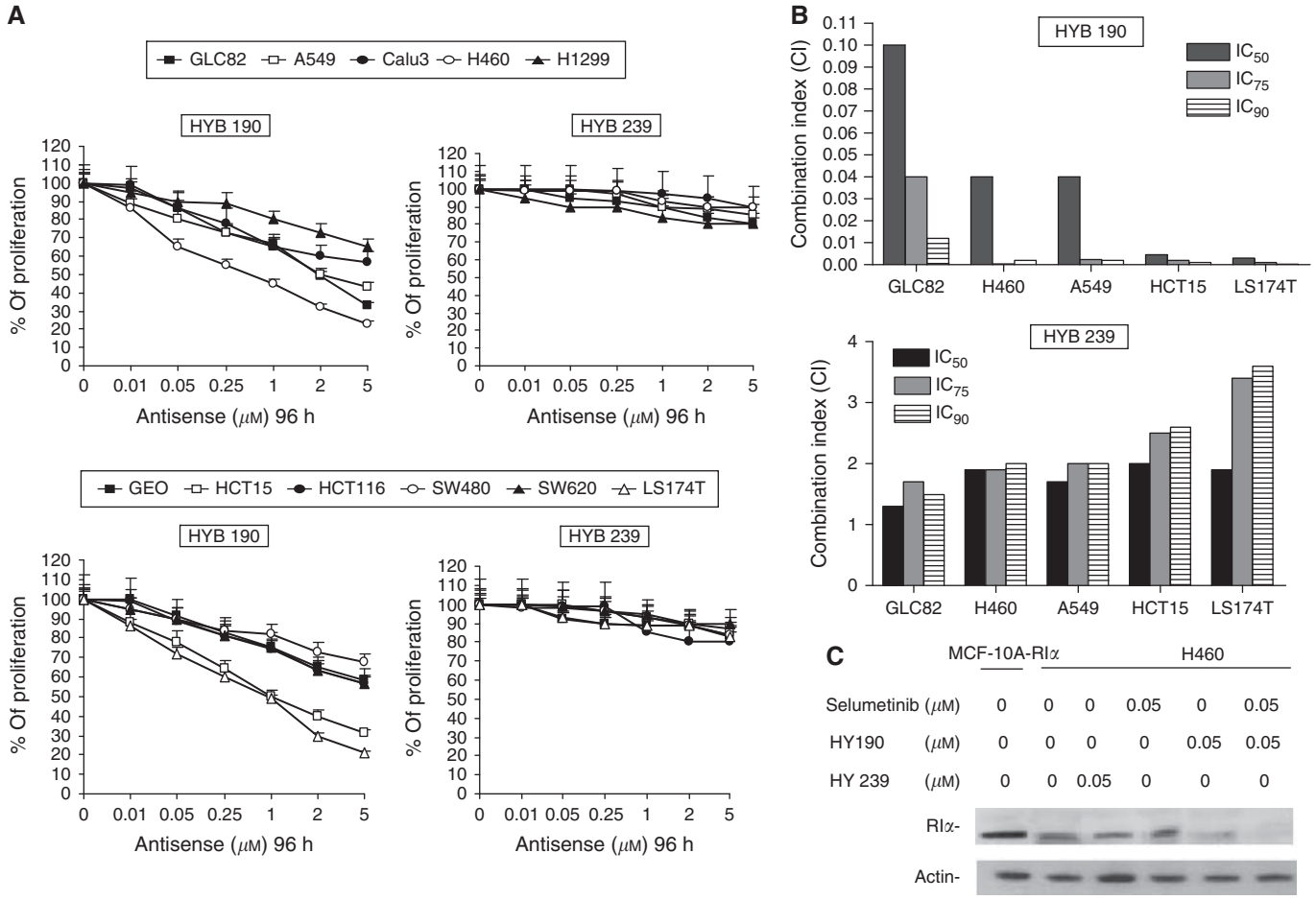

Figure 6 RIα HYB 190 antisense restores cancer cell sensitivity to MEK inhibition. (**A**) Cancer cells were treated with increasing concentrations of RIα antisense HYB 190 and its control sequence HYB 239 (range, 0.01–5 μM) for 96 h in different cancer cell lines and evaluated for proliferation by MTT staining, as described in Materials and Methods. The results are average ± s.d. of three independent experiments each done in duplicate. (**B**) Cancer cells were treated with different concentrations of selumetinib plus RIα antisense HYB 190 or HYB 239 as described in Materials and Methods. Experiments were done in triplicate. CI values were calculated according to Chou and Talalay model for drug interactions using the CalcuSyn software. (**C**) H460 cancer cells were treated with selumetinib, HYB 190, HYB 239, or selumetinib in combination with HYB 190 or HYB 239 at the indicated concentrations for 4 days. The cell lysates were immunoblotted with specific anti-RIα monoclonal monoantibody, as described in Materials and Methods.

oligonucleotide HYB 190, oligonucleotide HYB 239, selumetinib, and combinations. Compared with untreated H460 cells, RIα levels were substantially unchanged, even in cells treated with a higher dose of the control oligonucleotide HYB 239 (1 μM) and selumetinib (5 μM). However, reduction of RIα expression was seen when H460 cells were treated with oligonucleotide HYB 190 (Figure 6C). Moreover, a complete inhibition of RIα expression was seen in the combination treatment (Figure 6C).

We finally evaluated whether the combined inhibition of both PKA and MEK pathways would have antitumour activity *in vivo* in selumetinib-resistant HCT15 and H460 xenografts (Figure 7). At day 50 from cancer cell injection, the mean tumour volume in mice bearing HCT15 and H460 tumour xenografts and treated with selumetinib, 25 mg kg^{-1}, and 8-Cl-cAMP, 0.5 mg kg^{-1}, were 20% and 16%, respectively, as compared with control untreated mice.

DISCUSSION

Advances in the understanding of cancer biology have led to the development of novel and more selective anticancer therapies that are aimed to target specific cancer cell signalling pathways. In this respect, cancer patient selection is a key issue for the optimal use of these drugs. Therefore, identification of biomarkers that could be used to predict response to targeted agents is a crucial challenge in cancer drug development. The key role of the RAS/RAF/MEK/ERK signalling pathway in cancer cell biology and its potential as a therapeutic target in human cancer has been well established in preclinical models and clinical trials (Adjei *et al*, 2008; Balmanno *et al*, 2009; Bennouna *et al*, 2011; Bekaii-Saab *et al*, 2011; Dai *et al*, 2011; Dry *et al*, 2010; Hainsworth *et al*, 2010; Tendler *et al*, 2010; O'Nail *et al*, 2011). Highly selective small molecule MEK inhibitors have shown clinical activity in different cancers including colon and lung cancer in early clinical trials (Hainsworth *et al*, 2010; Bennouna *et al*, 2011).

In this study, we have used selumetinib, a selective inhibitor of MEK1/2 kinases, in a panel of five human NSCLC and six human CRC cell lines. We observed a wide range of *in-vitro* sensitivity to selumetinib. We considered selumetinib-sensitive cancer cell lines those in which the *in-vitro* IC_{50} for cell growth inhibition was >1 μM. Cell growth inhibition in selumetinib-sensitive cancer cell lines was paralleled by the induction of apoptosis, suggesting a cytotoxic rather than a cytostatic effect of selumetinib. These data are consistent with previous studies that demonstrated that selumetinib-induced apoptosis is mediated by activating the caspase pathways (Huynh *et al*, 2007b). Moreover, the inability of selumetinib to completely inhibit the phosphorylation of MEK1/2 and MAPK in selumetinib-resistant cancer cell lines suggests that

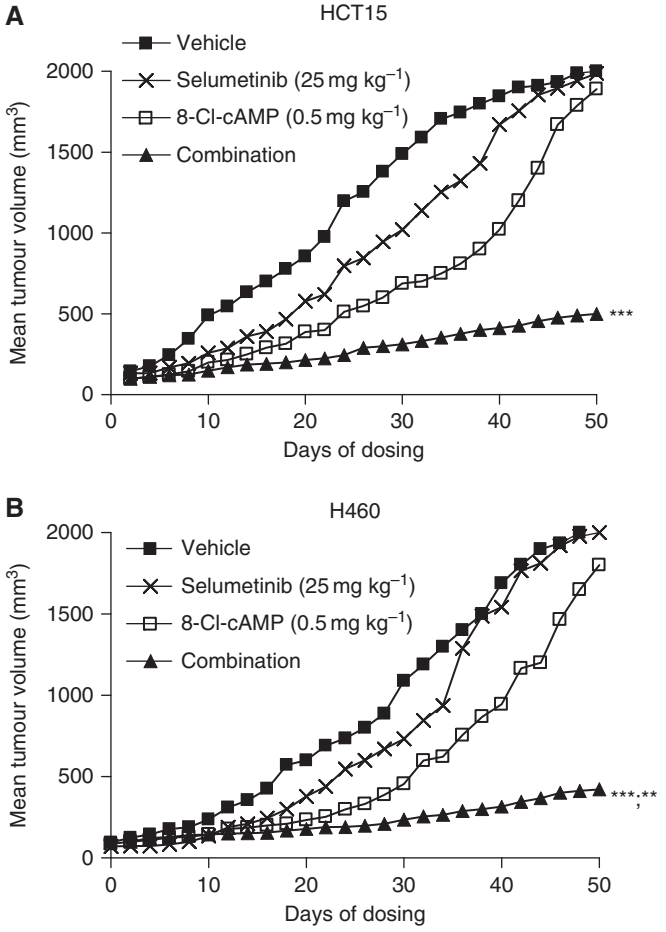

Figure 7 Combined treatment with selumetinib and 8-Cl-cAMP significantly inhibit tumour growth in selumetinib-resistant human tumour xenograft models. (**A**) HCT15 and (**B**) H460 cells were grown as tumour xenografts in nude mice. After tumour establishment (100–150 mm^3), mice were treated with selumetinib (25 mg kg^{-1}; oral gavage), twice a day (BID), 8-Cl-cAMP (0.5 mg kg^{-1}; intraperitoneal injection), twice a week or the combination of both drugs for 21 days. Animals were killed when tumours achieved 2000 mm^3 in size. $^{**}P<0.005$; $^{***}P<0.0005$.

the activation of alternative signalling pathways may be responsible of this effect.

We have extensively searched in the panel of NSCLC and CRC cells for mutations of genes coding for proteins involved in the intracellular signalling pathways regulating survival and proliferation and for the expression of the corresponding proteins in an attempt to identify different molecular patterns which could predict sensitivity or resistance to MEK inhibition by selumetinib. No correlation was found between the presence of gene mutations (*KRAS, NRAS, BRAF, MEK 1* and *2, p53, PI3KCA, EGFR, PTEN*) or protein expression and/or functional activation (MEK, MAPK, RAS, AKT) and sensitivity to selumetinib.

Activation of oncogenes or inactivation of tumour suppressor genes often results in a complex regulation of different cell signalling pathways. Therefore, gene expression profiles could provide more comprehensive means by which to assess the functional consequence of gene mutations and, therefore, may be a more effective tool for a personalised therapeutic approach. Although there are examples for which pathway activation and drug response can be predicted by a single oncogene mutation, it seems more likely that genomic analyses will be necessary to accurately predict response to molecular targeted agents (Lynch *et al*, 2004; Paez *et al*, 2004). Analysis of gene expression profiles in the panel of NSCLC and CRC cell lines identified a number of genes whose expression was upregulated or downregulated in selumetinib-resistant cancer cell lines as compared with selumetinib-sensitive ones. Interestingly, several genes which code for proteins that are key regulators of the cAMP-dependent PKA pathway resulted upregulated in selumetinib-resistant cancer cells.

PKA is an intracellular enzyme with serine-threonine kinase activity that has a key role in cell growth and differentiation. The PKA holoenzyme is a tetramer formed of two regulatory (R) subunits and two catalytic (C) subunits. Upon cAMP binding to the R subunits, the active C subunit is released and activated (Taylor *et al*, 1990). PKA is also involved in neoplastic transformation. In this respect, type I PKA (PKAI), which contains the RIα regulatory subunit, is generally upregulated in human cancer cell lines and primary tumours and is induced following transformation by certain oncogenes, such as *RAS* (Cho-Chung *et al*, 1995). Moreover, PKAI overexpression has been correlated with poor prognosis in cancer patients (Miller *et al*, 1993). Inhibition of PKAI expression and function by specific pharmacologic agents such as the site-selective cAMP analogue 8-Cl-cAMP induces growth inhibition *in vitro* and antitumour activity *in vivo* in various human cancer cell lines (Rohlff *et al*, 1993; Tagliaferri *et al*, 1988). Experimental evidence has been provided on a functional link between EGFR/RAS-RAF-MEK-ERK pathway and PKAI expression and activity (Ciardiello *et al*, 1996; Tortora and Ciardiello, 2000). The interaction between EGFR and PKAI occurs through direct binding of the RIα subunit to the Grb2 adaptor protein. Therefore, PKAI seems to function downstream to the EGFR, and experimental evidence suggests that PKAI is acting upstream to the MAPK pathway (Tortora *et al*, 1997b). In particular, PKAI provides a relevant contribution to the propagation of EGFR-activated mitogenic intracellular signalling. In fact, overexpression of PKAI in MCF-l0A human breast cells determines a constitutive activation of MAPK, mimicking the effect of EGF addition to quiescent MCF-10A cells. In contrast, inhibition of PKAI-mediated signalling by 8-Cl-cAMP significantly reduces MAPK activation in EGF-stimulated MCF- 10A cells (Tortora *et al*, 1997b). The combined blockade of EGFR and PKAI with selective inhibitors, such as the anti-EGFR blocking monoclonal antibody cetuximab and 8-Cl-cAMP, has a cooperative antitumour activity on human cancer cell lines *in vitro* and *in vivo* (Ciardiello *et al*, 1996). A role of PKAI in neoplastic transformation could be mediated either by the functional and structural connect with ERGF pathway and/or by its relationship with other signalling molecules such as bcl-2-dependent apoptotic pathway and such as tumour-induced neoangiogenesis (Tortora and Ciardiello, 2000).

In the present study, we have shown that treatment with 8-Cl-cAMP, a cAMP analogue that specifically inhibits PKAI, is able to overcome the resistance to MEK inhibition in selumetinib-resistant cancer cell lines both *in vitro* and *in vivo*. These results suggest that the PKA pathway could be activated in human cancer cells with intrinsic resistance to selective MEK inhibitors and represents a rationale for the investigation of combining MEK and PKA inhibitors in cancer treatment.

ACKNOWLEDGEMENTS

This research has been supported by a grant from the Associazione Italiana per la Ricerca sul Cancro (AIRC), Milan, Italy. T Troiani is the recipient of an ESMO Translational Research Fellowship and this is a major research project during her fellowship program.

Conflict of interest

The authors declare no conflict of interest.

Supplementary Information accompanies the paper on British Journal of Cancer website (http://www.nature.com/bjc)

REFERENCES

Adjei AA (2001) Blocking oncogenic Ras signaling for cancer therapy. *J Natl Cancer Inst* **93**: 1062–1074

Adjei AA, Cohen RB, Franklin WB, Morris C, Wilson D, Molina JR Hanson LJ, Gore L, Chow L, Leong S, Maloney L, Gordon G, Simmons H, Marlow A, Litwiler K, Brown S, Poch G, Kane K, Haney J, Eckhardt SG (2008) Phase I pharmacokinetic and pharmacodynamic study of the oral, small-molecule mitogen-activated protein kinase 1/2 inhibitor AZD6244 (ARRY-142886) in patients with advanced cancers. *J Clin Oncol* **26**: 2139–2146

Adjei AA, Hidalgo M (2005) Intracellular signal transduction pathway proteins as targets for cancer therapy. *J Clin Oncol* **23**: 5386–5403

Agrawal S, Jiang Z, Zhao Q, Shaw D, Cai Q, Roskey A, Channavajjala L, Saxinger C, Zhang R (1997) Mixed backbone oligonucleotides as second generation antisense oligonucleotides: *in vitro* and *in vivo* studies. *Proc Natl Acad Sci USA* **94**: 2620–2625

Allegra CJ, Jessup JM, Somerfield MR, Hamilton SR, Hammond EH Hayes DF, McAllister PK, Morton RF, Schilsky RL (2009) American Society of Clinical Oncology provisional clinical opinion: testing for KRAS gene mutations in patients with metastatic colorectal carcinoma to predict response to anti-epidermal growth factor receptor monoclonal antibody therapy. *J Clin Oncol* **27**: 2091–2096

Altucci L, Leibowitz MD, Ogilvie KM, de Lera AR, Gronemeyer H (2007) RAR and RXR modulation in cancer and metabolic disease. *Nat Rev Drug Discov* **6**: 793–810

Balmanno K, Chell SD, Gillings AS, Hayat S, Cook SJ (2009) Intrinsic resistance to the MEK1/2 inhibitor AZD6244 (ARRY-142886) is associated with weak ERK1/2 signalling and/or strong PI3K signalling in colorectal cancer cell lines. *Int J Cancer* **125**: 2332–2341

Bekaii-Saab T, Phelps MA, Li X, Saji M, Goff L, Kauh JS, O'Neil BH Balsom S, Balint C, Liersemann R, Vasko VV, Bloomston M, Marsh W, Doyle LA, Ellison G, Grever M, Ringel MD, Villalona-Calero MA (2011) Multi-institutional phase II study of selumetinib in patients with metastatic biliary cancers. *J Clin Oncol* **29**: 2357–2363

Bennouna J, Lang I, Valladares-Ayerbes M, Boer K, Adenis A, Escudero P, Kim TY, Pover GM, Morris CD, Douillard JY (2011) A phase II, open-label, randomized study to assess the efficacy and safety of the MEK1/2 inhibitor AZD6244 (ARRY-142886) versus capecitabine monotherapy in patients with colorectal cancer who have failed one or two prior chemotherapeutic regimens. *Invest New Drugs* **29**: 1021–1028

Brose MS, Volpe P, Feldman M, Kumar M, Rishi I, Gerrero R, Einhorn E, Herlyn M, Minna J, Nicholson A, Roth JA, Albelda SM, Davies H, Cox C, Brignell G, Stephens P, Futreal PA, Wooster R, Stratton MR, Weber BL (2002) BRAF and RAS mutations in human lung cancer and melanoma. *Cancer Res* **62**: 6997–7000

Cho-Chung YS, Pepe S, Clair T, Budillon A, Nesterova M (1995) cAMP-dependent protein kinase: role in normal and malignant growth. *Crit Rev Oncol Hematol* **21**: 33–61

Ciardiello F, Damiano V, Bianco R, Bianco C, Fontanini G, De Laurentiis M, De Placido S, Mendelsohn J, Bianco AR, Tortora G (1996) Antitumor activity of combined blockade of epidermal growth factor receptor and protein kinase A. *J Natl Cancer Inst* **88**: 1770–1776

Dai D, Meng J, Peyton M, Girard L, Bornmann WG, Ji L, Minna JD, Fang B, Roth JA (2011) STAT3 mediates resistance to MEK inhibitor through microRNA miR-17. *Cancer Res* **71**: 3658–3668

Davies B, Logie A, McKay J, Martin P, Steele S, Jenkins R, Cockerill M, Cartlidge S, Smith PD (2007) AZD6244 (ARRY-142886), a potent inhibitor of mitogen activated protein kinase/extracellular signal regulated kinase kinase 1/2 kinases: mechanism of action *in vivo*, pharmacokinetic/pharmacodynamic relationship, and potential for combination in preclinical models. *Mol Cancer Ther* **6**: 2209–2219

De Roock W, Claes B, Bernasconi D, De Schutter J, Biesmans B Fountzilas G, Kalogeras KT, Kotoula V, Papamichael D Laurent-Puig P, Penault-Llorca F, Rougier P, Vincenzi B, Santini D, Tonini G, Cappuzzo F, Frattini M, Molinari F, Saletti P, De Dosso S, Martini M, Bardelli A, Siena S, Sartore-Bianchi A, Tabernero J Macarulla T, Di Fiore F, Gangloff AO, Ciardiello F, Pfeiffer P, Qvortrup C, Hansen TP, Van Cutsem E, Piessevaux H, Lambrechts D, Delorenzi M, Tejpar S (2010) Effects of KRAS, BRAF, NRAS, and PIK3CA mutations on the efficacy of cetuximab plus chemotherapy in chemotherapy-refractory metastatic colorectal cancer: a retrospective consortium analysis. *Lancet Oncol* **11**: 753–762

Downward J (2006) Cancer biology: signatures guide drug choice. *Nature* **439**: 274–275

Dry JR, Pavey S, Pratilas CA, Harbron C, Runswick S, Hodgson D Chresta C, McCormack R, Byrne N, Cockerill M, Graham A, Beran G, Cassidy A, Haggerty C, Brown H, Ellison G, Dering J, Taylor BS, Stark M, Bonazzi V, Ravishankar S, Packer L, Xing F, Solit DB, Finn RS, Rosen N, Hayward NK, French T, Smith PD (2010) Transcriptional pathway signatures predict MEK addiction and response to selumetinib (AZD6244). *Cancer Res* **70**: 2264–2273

Garon EB, Finn RS, Hosmer W, ering J, Ginther C, Adhami S, Kamranpour N, Pitts S, Desai A, Elashoff D, French T, Smith P, Slamon DJ (2010) Identification of common predictive markers of *in vitro* response to the Mek inhibitor selumetinib (AZD6244; ARRY-142886) in human breast cancer and non-small cell lung cancer cell lines. *Mol Cancer Ther* **9**: 1985–1994

Hahn WC, Weinberg RA (2002) Modelling the molecular circuitry of cancer. *Nat Rev Cancer* **2**: 331–341

Hainsworth JD, Cebotaru CL, Kanarev V, Ciuleanu TE, Damyanov D Stella P, Ganchev H, Pover G, Morris C, Tzekova V (2010) A phase II, open-label, randomized study to assess the efficacy and safety of AZD6244 (ARRY-142886) versus pemetrexed in patients with non-small cell lung cancer who have failed one or two prior chemotherapeutic regimens. *J Thorac Oncol* **5**: 1630–1636

Hanahan D, Weinberg RA (2011) Hallmarks of cancer: next generation *Cell* **144**: 646–674

Hoshino R, Chatani Y, Yamori T, Tsuruo T, Oka H, Yoshida O, Shimada Y, Ari-i S, Wada H, Fujimoto J, Kohno M (1999) Constitutive activation of the 41-/43-kDa mitogen-activated protein kinase signaling pathway in human tumors. *Oncogene* **18**: 813–822

Huynh H, Chow PKH, Soo KC (2007a) AZD6244 and doxorubicin induce growth suppression and apoptosis in mouse models of hepatocellular carcinoma. *Mol Cancer Ther* **6**: 2468–2476

Huynh H, Soo KC, Chow PK, Tran E (2007b) Targeted inhibition of the extracellular signal-regulated kinase pathway with AZD6244 (ARRAY-142886) in the treatment of hepatocellular carcinoma. *Mol Cancer Ther* **6**: 138–146

Lievre A, Bachet JB, Le Corre D, Boige V, Landi B, Emile JF, Côté JF, Tomasic G, Penna C, Ducreux M, Rougier P, Penault-Llorca F, Laurent-Puig P (2006) KRAS mutation status is predictive of response to cetuximab therapy in colorectal cancer. *Cancer Res* **66**: 3992–3995

Lynch TJ, Bell DW, Sordella R, Gurubhagavatula S, Okimoto RA, Brannigan BW, Harris PL, Haserlat SM, Supko JG, Haluska FG, Louis DN, Christiani DC, Settleman J, Haber DA (2004) Activating mutations in the epidermal growth factor receptor underlying responsiveness of non-small-cell lung cancer to gefitinib. *N Engl J Med* **350**: 2129–2139

Massarelli E, Varella-Garcia M, Tang X, Xavier AC, Ozburn NC, Liu DD, Bekele BN, Herbst RS, Wistuba (2007) KRAS mutation is an important predictor of resistance to therapy with epidermal growth factor receptor tyrosine kinase inhibitors in non-small-cell lung cancer. *Clin Cancer Res* **13**: 2890–2896

Meng J, Dai B, Fang B, Bornmann WG, Sun D, Peng Z, Herbst RS, Papadimitrakopoulou V, Minna JD, Peyton M, Roth JA (2010) Combination treatment with MEK and AKT inhibitors is more effective than each drug alone in human non-small cell lung cancer *in vitro* and *in vivo*. *PLoS One* **5**: e141240

Meng J, Peng H, Dai B, Guo W, Wang L, Ji L, Minna JD, Chresta CM, Smith PD, Fang B, Roth JA (2009) High level of AKT activity is associated with resistance to MEK inhibitor AZD6244 (ARRAY-142886). *Cancer Biol Ther* **8**: 2073–2080

Miller WR, Watson DMA, Jack W, Chetty U, Elton RA (1993) Tumor cyclic AMP binding proteins: an independent prognostic factor for disease recurrence and survival in breast cancer. *Breast Cancer Res Treat* **26**: 89–94

Morgillo F, Cascone T, D'aiuto E, Martinelli E, Troiani T, Saintigny P De Palma R, Heymach JV, Berrino L, Tuccillo C, Ciardiello F (2011) Antitumor efficacy of MEK inhibitors in human lung cancer cells and their derivatives with acquired resistance to different tyrosine kinase inhibitors. *Br J Cancer* **105**: 382–392

Mueller H, Flury N, Eppenberger-Castori S, Kueng W, David F, Eppenberger U (2000) Potential prognostic value of mitogen-activated protein kinase activity for disease-free survival of primary breast cancer patients. *Int J Cancer* **89**: 384–388

Naviglio S, Caraglia M, Abbruzzese A, Chiosi E, Di Gesto D, Marra M, Romano M, Sorrentino A, Sorvillo L, Spina A, Illiano G (2009) Protein

Kinase A as a biological target in cancer therapy. *Expert Opin Ther Targets* **13**: 83–92

Nesterova M, Cho-Chung YS (1995) A single-injection protein kinase A-directed antisense treatment to inhibit tumour growth. *Nat Med* **1**: 528–533

O'Nail BH, Goff LW, Kauh JS, Strosberg JR, Bekaii-Saab TS, Lee RM, Kazi A, Moore DT, Learoyd M, Lush RM, Sebti SM, Sullivan DM (2011) Phase II study of the mitogen-activated protein kinase 1/2 inhibitor selumetinib in patient with advanced hepatocellular carcinoma. *J Clin Oncol* **29**: 235–256

Paez JG, Janne PA, Lee JC, Tracy S, Greulich H, Gabriel S, Herman P, Kaye FJ, Lindeman N, Boggon TJ, Naoki K, Sasaki H, Fujii Y, Eck MJ, Sellers WR, Johnson BE, Meyerson M (2004) EGFR mutations in lung cancer: correlation with clinical response to gefitinib therapy. *Science* **304**: 1497–1500

Pao W, Wang TY, Riely GJ, Miller VA, Pan Q, Ladanyi M, Zakowski MF, Heelan RT, Kris MG, Varmus HE (2005) KRAS mutations and primary resistance of lung adenocarcinomas to gefitinib or erlotinib. *PLoS Med* **2**: e17

Rohlff C, Clair T, Cho-Chung YS (1993) 8-Cl-cAMP induces truncation and down-regulation of the RIα subunit and up-regulation of the RIIβ subunit of cAMP-dependent protein kinase leading to type II holoenzyme-dependent growth inhibition and differentiation of HL-6 leukemia cells. *J Biol Chem* **268**: 5774–5782

Sebolt-Leopold JS (2004) MEK inhibitors: a therapeutic approach to targeting the Ras-MAP kinase pathway in tumors. *Curr Pharm Des* **10**: 1907–1914

Shannon AM, Telfer BA, Smith PD, Babur M, Logie A, Wilkinson RW, Debray C, Stratford IJ, Williams KJ, Wedge SR (2009) The mitogen-activated protein/extracellular signal-regulated kinase kinase 1/2 inhibitor AZD6244 (ARRY-142886) enhances the radiation responsiveness of lung and colorectal tumor xenografts. *Clin Cancer Res* **15**: 6619–6629

Tagliaferri P, Katsaros D, Clair T, Ally S, Tortora G, Neckers L Rubalcava B, Parandoosh Z, Chang YA, Revankar GR, Crabtree GW, Robins RK, Cho-Chung YS (1988) Synergistic inhibition of growth of breast and colon human cancer cell lines by site-selective cAMP analogs. *Cancer Res* **48**: 1642–1650

Tasken K, Skalhegg BS, Tasken KA, Solberg R, Knutsen HK, Levy FO, Sandberg M, Orstavik S, Larsen T, Johansen AK, Vang T, Schrader HP, Reinton NT, Torgersen KM, Hansson V, Jahnsen T (1997) Structure, function, and regulation of human cAMP-dependent protein kinases. *Adv Second Messenger Phosphoprotein Res* **31**: 191–204

Taylor SS, Buechler JA, Yonemoto W (1990) cAMP-dependent protein kinase: framework for a diverse family of regulatory enzymes. *Annu Rev Biochem* **59**: 971–1005

Tentler JJ, Nallapareddy S, Tan AC, Spreafico A, Pitts TM, Morelli MP, Selby HM, Kachaeva MI, Flanigan SA, Kulikowski GN, Leong S, Arcaroli JJ, Messersmith WA, Eckhardt SG (2010) Identification of predictive biomarkers of response to the MEK1/2 inhibitor selumetinib (AZD6244) in K-ras mutated colorectal cancer. *Mol Cancer Ther* **9**: 3351–3362

Tortora G, Caputo R, Damiano V, Bianco R, Pepe S, Bianco AR, Jiang Z, Agrawal S, Ciardiello F (1997a) Synergistic inhibition of human cancer cell growth by cytotoxic drugs and mixed backbone antisense oligonucleotide targeting protein kinase A. *Proc Natl Acad Sci USA* **94**: 12586–12591

Tortora G, Ciardiello F (2000) Targeting of the epidermal growth factor and protein kinase A: molecular basis and therapeutic applications. *Ann Oncol* **11**: 777–783

Tortora G, Damiano V, Bianco C, Baldassarre G, Bianco AR, Lanfrancone L, Pelicci PG, Ciardiello F (1997b) The RIα subunit of protein kinase A (PKA) binds to Grb2 and allows PKA interaction with the activated EGFR-receptor. *Oncogene* **14**: 923–928

Yeh TC, Marsh V, Bernat BA, Ballard J, Colwell H, Evans RJ, Parry J, Smith D, Brandhuber BJ, Gross S, Marlow A, Hurley B, Lyssikatos J, Lee PA, Winkler JD, Koch K, Wallace E (2007) Biological characterization of ARRY-142886 (AZD6244), a potent, highly selective mitogen-activated protein kinase 1/2 inhibitor. *Clin Cancer Res* **13**: 1576–1583

Yokozaki H, Budillon A, Tortora G, Meissner S, Beaucage S, Miki K, Cho-Chung YS (1993) An antisense oligodeoxynucleotide that depletes RIα subunit of cyclic AMP-dependent protein kinase induces growth inhibition in human cancer cells. *Cancer Res* **53**: 868–872

Yuen ST, Davies H, Chan TL, Ho JW, Bignell GR, Cox C, Stephens P, Edkins S, Tsui WW, Chan AS, Futreal PA, Stratton MR, Wooster R, Leung SY (2002) Similarity of the phenotypic patterns associated with BRAF and KRAS mutations in colorectal neoplasia. *Cancer Res* **62**: 6997–7000